

# Phase-controlled proximity-effect in ferromagnetic Josephson junctions: calculation of DOS and electronic specific heat

Mohammad Alidoust,<sup>1</sup> Jacob Linder,<sup>2</sup> Gholamreza Rashedi,<sup>1</sup> and Asle Sudbø<sup>2</sup>

<sup>1</sup>*Department of Physics, Faculty of Sciences, University of Isfahan, Hezar Jerib Avenue, Isfahan 81746-73441, Iran*

<sup>2</sup>*Department of Physics, Norwegian University of Science and Technology, N-7491 Trondheim, Norway*

(Dated: Received June 5, 2017)

We study the thermodynamic properties of a dirty ferromagnetic S|F|S Josephson junction with  $s$ -wave superconducting leads in the low-temperature regime. We employ a full numerical solution with a set of realistic parameters and boundary conditions, considering both a uniform and non-uniform exchange field in the form of a Bloch domain wall ferromagnetic layer. The influence of spin-active interfaces is incorporated via a microscopic approach. We mainly focus on how the electronic specific heat and density of states (DOS) of such a system is affected by the *proximity effect*, which may be tuned via the superconducting phase difference. Our main result is that it is possible to *strongly modify the electronic specific heat* of the system by changing the phase difference between the two superconducting leads from 0 up to nearly  $\pi$  at low temperatures. An enhancement of the specific heat will occur for small values  $h \simeq \Delta$  of the exchange field, while for large values of  $h$  the specific heat is suppressed by increasing the phase difference between the superconducting leads. These results are all explained in terms of the proximity-altered DOS in the ferromagnetic region, and we discuss possible methods for experimental detection of the predicted effect.

PACS numbers: 85.25.Dq,74.25.Bt,74.45.+c,74.78.Na

## I. INTRODUCTION

In recent years, due to the important role of hybrid structures with superconducting and magnetic layers in vital circuit-elements like transistors and high-resolution devices like detectors, such structures has attracted much attention from the research community. In this way, several interesting phenomena of such systems have been predicted both in the dirty and clean limits of transport, and subsequently been observed in experiments: non-monotonic dependence of the critical temperature  $T_c$  in S|F hybrid structures on the thickness of F layer,<sup>1,2,3,4,5</sup> the  $0$ - $\pi$  transitions in S|F|S junctions,<sup>6,7,8</sup> and the appearance of odd-frequency pairing correlations<sup>9,10</sup> just to mention a few. The main cause of the appearance of these interesting phenomena is the *proximity effect* between the superconductor and the ferromagnet, where Cooper pairs leak from the superconducting side to the ferromagnetic layer. S|F|S junctions are routinely fabricated by experimentalists these days, and currently such hybrid structures are intensely investigated due to their potential both in terms of functionality<sup>11</sup> and novel fundamental physics that may be explored.<sup>12,13</sup>

In the context of applications, studies of the thermodynamic properties of superconductors have mostly focused on electron cooling properties<sup>14</sup>, although recently the influence of the proximity effect on the entropy production in a non-magnetic Josephson junction was investigated<sup>15</sup>. A key to understanding the thermodynamic properties of a system is the behavior of the DOS near Fermi level, and any control parameter that can adjust the DOS in an efficient and well-defined manner would offer significant advantages with respect to tailoring desired thermodynamic properties.

Very recently, it has been studied numerically<sup>16</sup> and demonstrated experimentally<sup>17</sup> how the density of states (DOS) may be altered controllably in such structures by creating a non-magnetic S|N|S Josephson junction and generating a super-

current. For a ferromagnetic Josephson junction, however, it remains to be clarified precisely how the DOS is influenced by the phase difference in the full proximity effect regime. A new feature which is expected to come into play for ferromagnetic Josephson junctions is the presence of odd-frequency superconducting correlations, which can induce a qualitative shift in the DOS from a low-energy minigap-structure<sup>18</sup> to an enhancement<sup>19</sup>.

In this paper, we show how it is possible to obtain a *huge enhancement of the specific heat* of a ferromagnetic Josephson junction at low temperatures, simply by tuning the superconducting phase difference by means of either a current or an external magnetic flux in a SQUID-like geometry. We demonstrate explicitly how the predicted effect occurs for a set of realistic experimental parameters, and how it persists even in the presence of an inhomogeneous magnetization texture such as a Bloch domain wall in the ferromagnet. We find that the enhancement of the specific heat is strongest for exchange fields  $h$  comparable in magnitude to the superconducting gap  $\Delta$ , i.e.  $h \simeq \Delta$ , whereas for higher exchange fields the effect eventually vanishes. Our findings can be verified experimentally by using calorimetry techniques or high-resolution thermometry,<sup>20</sup> and could have potential applications in devices utilizing an active tuning of the thermodynamic properties of nanoscale conductors. We underline that while it is well-known that the DOS in a Josephson junction is sensitive to the phase difference, our main result pertains to *the manner in which the DOS varies and the resulting consequences for the electronic specific heat of the junction*.

## II. THEORY

To investigate the physical properties of the S|F|S Josephson junction, one alternative is to solve the quasiclassical Eilenberger equation<sup>21,22</sup> to obtain the Green's functions. In

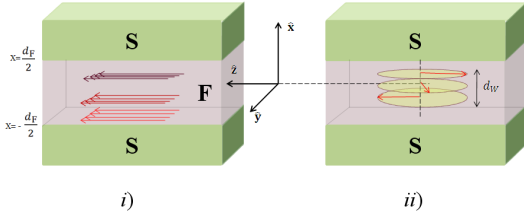


FIG. 1: (Color online) The S|F|S junction with *i*) uniform ferromagnet in the  $\hat{z}$  direction and *ii*) with a Bloch domain wall in the ferromagnet. The magnetization texture for the Néel wall would be obtained by replacing the  $x$ -component of the magnetization with an  $y$ -component in case *ii*). The red arrows show the magnetic moments in the F layer.

the diffusive limit, the Eilenberger equation reduces to a simpler set of equations known as the Usadel equations<sup>26</sup>. For numerical purposes, it is convenient to use a parameterization method for the Green's functions. One approach for the parameterization is the  $\theta$ -parameterization<sup>23</sup> as follows:

$$\hat{g} = \begin{pmatrix} M_0 c \underline{\sigma}_0 + (\mathbf{M} \cdot \underline{\sigma}) s & \rho^+ \\ \rho^- & -M_0 c \underline{\sigma}_0 - (\mathbf{M} \cdot \underline{\sigma})^* s \end{pmatrix}, \quad (1)$$

$$\rho^\pm = c [1(M_z \underline{\sigma}_2 - M_y \underline{\sigma}_3) \pm M_x \underline{\sigma}_0] \pm M_0 \underline{\sigma}_1 s,$$

where  $\underline{\sigma}_j$  are the identity ( $j = 0$ ) and Pauli ( $j = 1, 2, 3$ ) matrices, and

$$\underline{\sigma} = (\underline{\sigma}_1, \underline{\sigma}_2, \underline{\sigma}_3). \quad (2)$$

Also,  $s \equiv \sinh(\theta)$  and  $c \equiv \cosh(\theta)$ . The Green's function is then completely determined by the complex functions  $\theta$ ,  $M_0$ , and  $\mathbf{M}$  with the additional constraint  $M_0^2 - \mathbf{M}^2 = 1$  in order to satisfy  $\hat{g}^2 = \hat{1}$ . The other approach for a parameterization of the Green's functions is the Ricatti-parameterization<sup>24,25</sup>. We found that for our purposes in this paper, *i.e.* a full numerical investigation of the density of states and consequently the thermodynamic properties of a diffusive S|F|S junctions, this parameterization is much more numerically stable than the  $\theta$ -parameterization. The Ricatti-parameterization can read as follow:<sup>16,25</sup>

$$\hat{g} = \begin{pmatrix} \underline{\mathcal{N}}(1 - \underline{\gamma}\tilde{\gamma}) & 2\underline{\mathcal{N}}\underline{\gamma} \\ 2\underline{\tilde{\mathcal{N}}}\tilde{\gamma} & \underline{\tilde{\mathcal{N}}}(-1 + \tilde{\gamma}\gamma) \end{pmatrix}. \quad (3)$$

Here,  $\hat{g}^2 = \hat{1}$  since

$$\underline{\mathcal{N}} = (1 + \underline{\gamma}\tilde{\gamma})^{-1} \underline{\tilde{\mathcal{N}}} = (1 + \tilde{\gamma}\gamma)^{-1}. \quad (4)$$

We use  $\underline{\dots}$  for  $2 \times 2$  matrices and  $\hat{\dots}$  for  $4 \times 4$  matrices. In order to calculate the Green's function  $\hat{g}$ , we need to solve the Usadel equation<sup>26</sup> with appropriate boundary conditions at  $x = -d_F/2$  and  $x = d_F/2$ . We introduce the superconducting coherence length as  $\xi_S = \sqrt{D_S/\Delta_0}$ . Following the notation of Ref.<sup>27</sup>, the Usadel equation reads

$$D\partial(\hat{g}\partial\hat{g}) + \mathbb{1}[E\hat{\rho}_3 + \text{diag}[\mathbf{h} \cdot \underline{\sigma}, (\mathbf{h} \cdot \underline{\sigma})^T], \hat{g}] = 0, \quad (5)$$

and we employ the following realistic boundary conditions for all our computations in this paper:<sup>28</sup>

$$2\zeta d_F \hat{g} \partial \hat{g} = [\hat{g}_{\text{BCS}}(\phi), \hat{g}] + \mathbb{1}(G_S/G_T) [\text{diag}(\underline{\tau}_3, \underline{\tau}_3), \hat{g}] \quad (6)$$

at  $x = -d_F/2$ . Here,  $\partial \equiv \frac{\partial}{\partial x}$  and we defined  $\zeta = R_B/R_F$  as the ratio between the resistance of the barrier region and the resistance in the ferromagnetic film. The barrier conductance is given by  $G_T$ , whereas the parameter  $G_S$  describes the spin-dependent interfacial phase-shifts (spin-DIPS) taking place at the F side of the interface where the magnetization is assumed to lie in the  $yz$ -plane, being parallel to the  $z$ -axis at the interfaces. The boundary condition at  $x = d_F/2$  is obtained by letting  $G_S \rightarrow (-\tilde{G}_S)$  and  $\hat{g}_{\text{BCS}}(\phi) \rightarrow [-\hat{g}_{\text{BCS}}(-\phi)]$  in Eq. (6), where

$$\underline{\gamma}_{\text{BCS}}(\phi) = \mathbb{1}\underline{\tau}_2 s / (1 + c) e^{\mathbb{1}\phi/2},$$

$$\tilde{\underline{\gamma}}_{\text{BCS}}(\phi) = \underline{\gamma}_{\text{BCS}}(\phi) e^{-\mathbb{1}\phi}. \quad (7)$$

Above,  $\tilde{G}_S$  is allowed to be different from  $G_S$  in general. For instance, if the exchange field has opposite direction at the two interfaces due to the presence of a domain wall, one finds  $\tilde{G}_S = -G_S$ . The total superconducting phase difference is  $\phi$ , and we have defined  $s = \sinh(\vartheta)$ ,  $c = \cosh(\vartheta)$  with  $\vartheta = \text{atanh}(\Delta_0/E)$  using  $\Delta_0$  as the superconducting gap. Note that we use the bulk solution in the superconducting region, which is a good approximation when assuming that the superconducting region is much less disordered than the ferromagnet and when the interface transparency is small, as considered here. Effectively, the inverse proximity effect is thus ignored. We use units such that  $\hbar = k_B = 1$ .

The values of  $G_S$  and  $G_T$  may be calculated explicitly from a microscopic model, which allows one to characterize the transmission  $\{t_{n,\sigma}^j\}$  and reflection amplitudes  $\{r_{n,\sigma}^j\}$  on the  $j \in \{S, F\}$  side. Under the assumption of tunnel contacts and a weak ferromagnet, one obtains with a Dirac-like barrier model<sup>28,29,30</sup>

$$G_T = G_Q \sum_n T_n, \quad G_S = 2G_Q \sum_n \left( \rho_n^F - \frac{4\tau_n^S}{T_n} \right) \quad (8)$$

upon defining  $T_n = \sum_\sigma |t_{n,\sigma}^S|^2$ ,  $\rho_n^F = \text{Im}\{r_{n,\uparrow}^F (r_{n,\downarrow}^F)^*\}$  and  $\tau_n^S = \text{Im}\{t_{n,\uparrow}^S (t_{n,\downarrow}^S)^*\}$  and also for simplicity, we assume that the interface is characterized by  $N$  identical scattering channels and consequently omit the subscript 'n' in the summations.

To find the specific heat of the system, we need to calculate the local density of states normalized against its normal-state value

$$N(x, E, T, \phi) = \text{Tr}(\text{Re}[\underline{\mathcal{N}}(1 - \underline{\gamma}\tilde{\gamma})])/2. \quad (9)$$

We assume that the S electrodes are not influenced by the proximity effect, the total electronic specific heat ( $C_{\text{tot}}$ ) of the SFS junction can be determined by

$$C_{\text{tot}}(T, \phi) = C_F(T, \phi) + C_S(T). \quad (10)$$

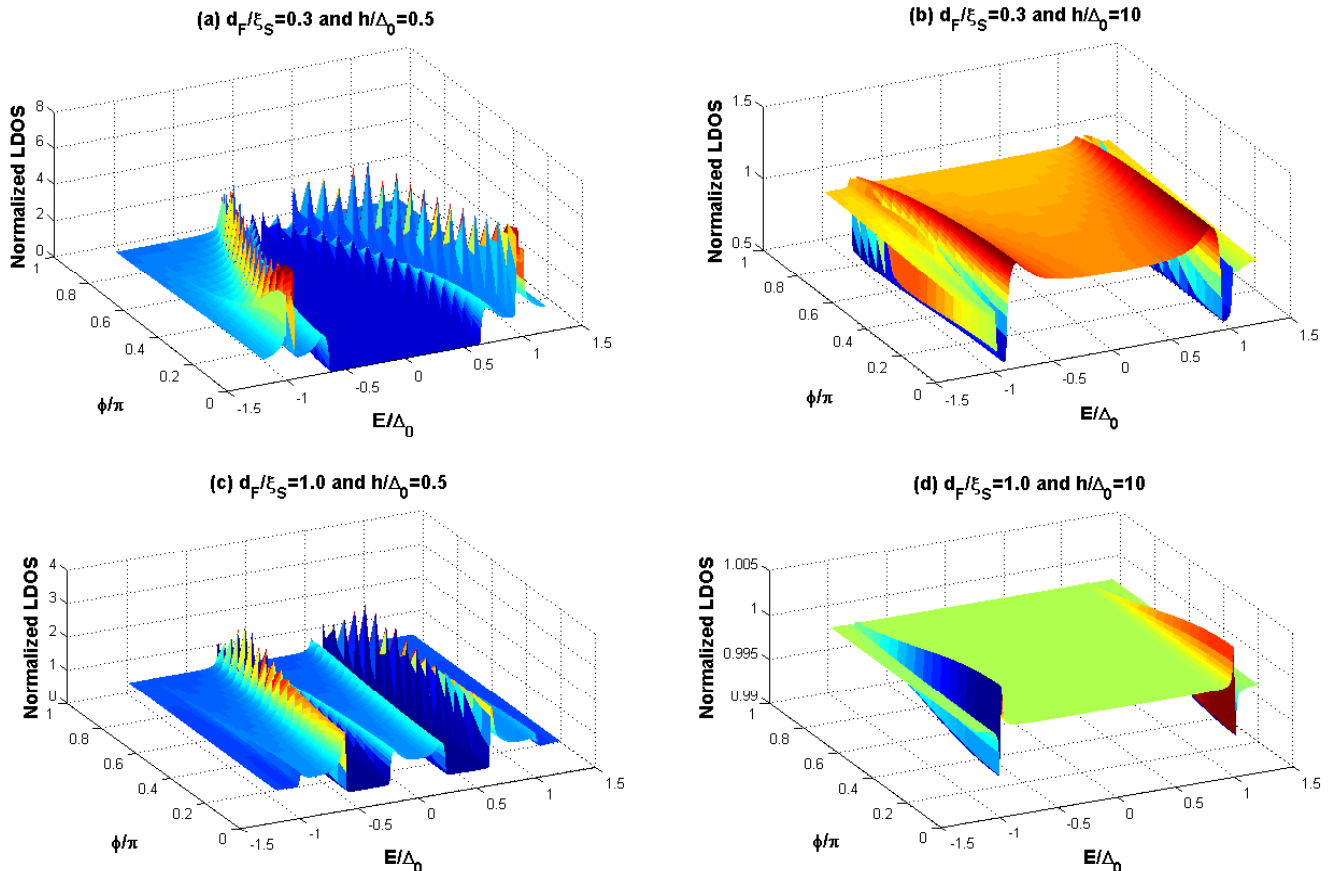


FIG. 2: (Color online) The normalized local density of states vs. energy and phase difference between two  $s$ -wave superconducting leads for a uniform magnetization texture. We have presented several values of the thickness of ferromagnetic layer  $d_F/\xi_S$  and exchange field  $h/\Delta_0$ , and the DOS is evaluated in the middle of the junction, *i.e.*  $x = 0$ .

Here,  $C_S(T)$  is the specific heat of superconducting plates while

$$C_F(T, \phi) = T \partial S_F(T, \phi) / \partial T, \quad (11)$$

is the specific heat of the ferromagnetic part of the junction. The entropy of the ferromagnet layer in the proximity system can be obtained from

$$S_F(T, \phi) = -(4/L) \int_{-L/2}^{L/2} dx \int_0^\infty dE N(x, E, T, \phi) \times \{f(E) \ln[f(E)] + [1 - f(E)] \ln[1 - f(E)]\}, \quad (12)$$

and  $f(E) = \{1 + \exp[E/T]\}^{-1}$  is the Fermi-Dirac quasiparticle distribution function at temperature  $T$ .

Since we employ a numerical solution, we have access to study the full proximity effect regime and also, in principle, an arbitrary spatial modulation  $h = h(x)$  of the exchange field. This is desirable in order to clarify effects associated with non-uniform ferromagnets, such as the presence of Bloch domain walls.

In this paper, we will consider two different types of magnetization textures: homogeneous magnetization and a Bloch domain wall structure as shown in the Fig. 1*i*) and *ii*), respectively. It is seen from Fig. 1 part *ii*) that for a domain wall structure, the magnetic moment has two components unlike the homogeneous type. The Bloch model is given by  $\mathbf{h} = h(\cos \theta \hat{y} + \sin \theta \hat{z})$  and its structure is shown in Fig. 1 part *ii*), where we defined  $\theta = -2 \arctan(x/d_W)^{25}$ , with  $d_W$  as the width of domain wall. Moreover, the center of the F layer is located at the origin  $x = 0$ . Below, we shall consider a domain wall of width  $d_W/d_F = 0.5$ , thus ensuring that the magnetization is fully aligned with the  $z$ -axis at the interfaces.

### III. RESULTS AND DISCUSSION

In this section, we present our main results of the paper, namely the manner in which the DOS of a S|F|S diffusive Josephson junction is altered in the presence of phase difference between two  $s$ -wave superconducting leads and consequently the behavior of the electronic specific heat of such junctions. We consider a ferromagnet with two types of mag-

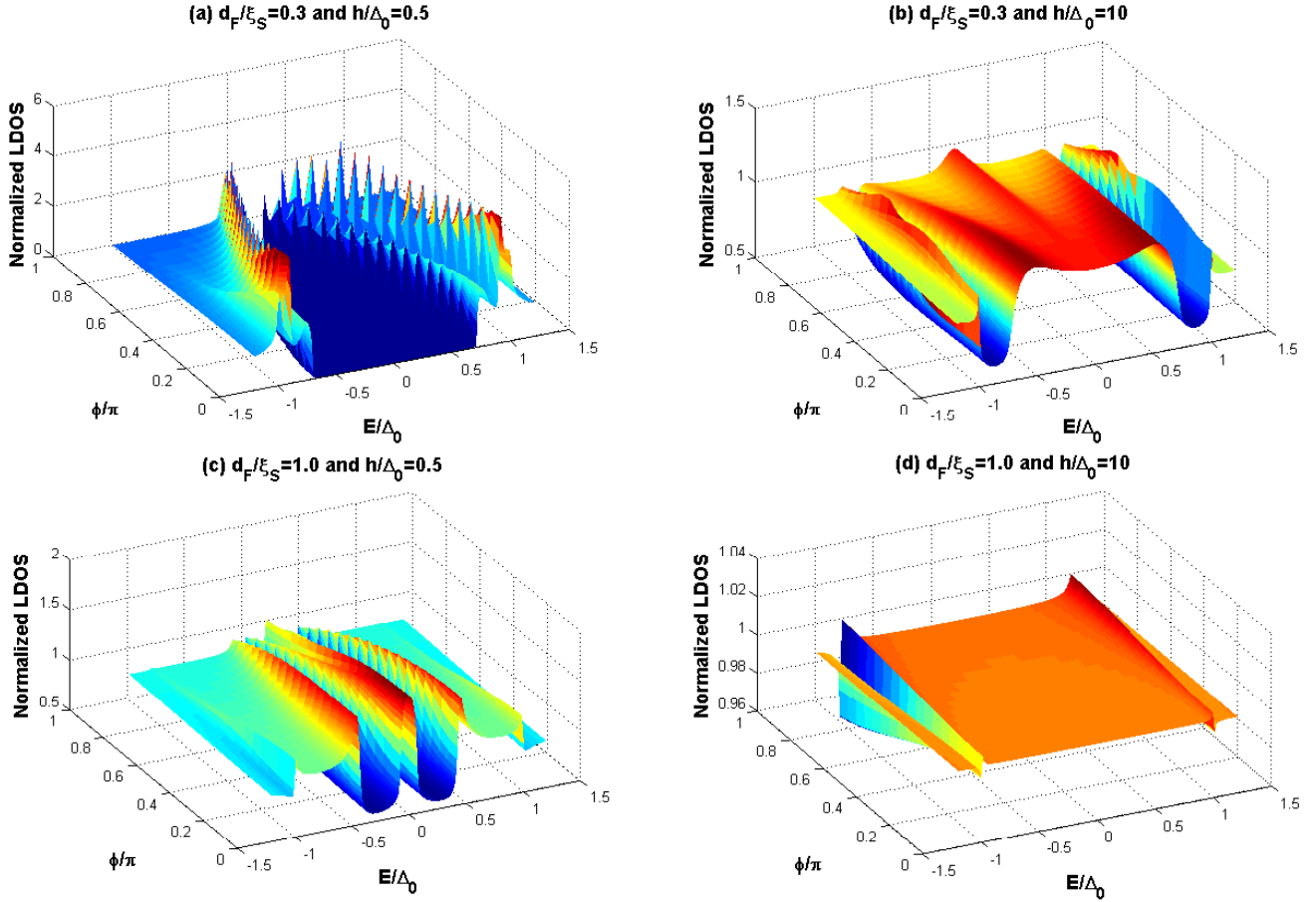


FIG. 3: (Color online) The normalized local density of states vs. energy and phase difference between two  $s$ -wave superconducting leads and inhomogeneous magnetization texture for several values of thickness of ferromagnetic layer  $d_F/\xi_S$  and exchange field  $h/\Delta_0$ . The DOS is evaluated in the middle of the junction, *i.e.*  $x = 0$ .

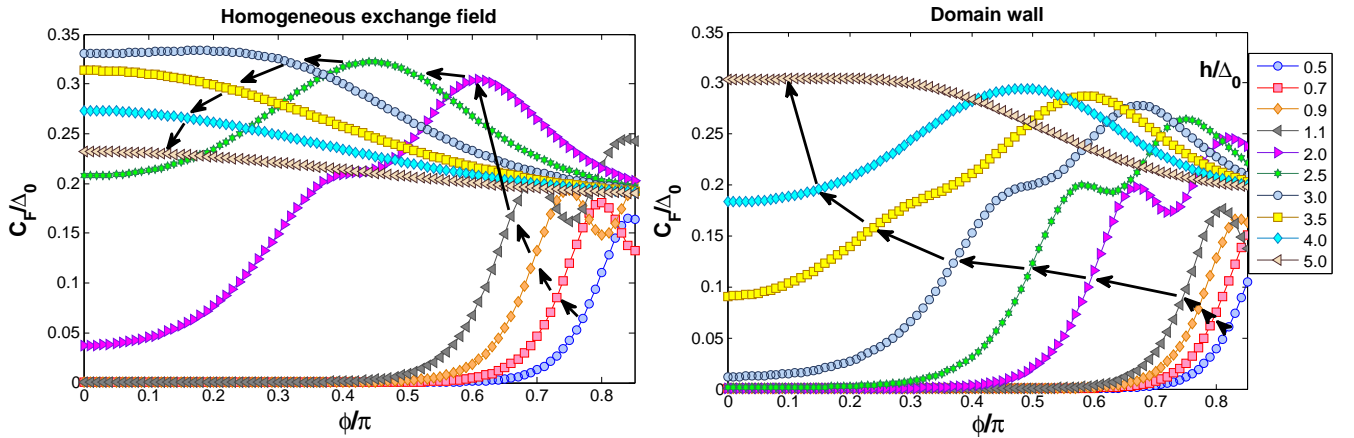


FIG. 4: (Color online) The normalized electronic specific heat of the diffusive S|F|S Josephson junction vs. phase difference between two  $s$ -wave superconducting leads with a ferromagnetic layer featuring a homogeneous (left panel) and inhomogeneous Bloch domain wall magnetization texture (right panel). The arrows indicate an increasing exchange field  $h$ .

netization texture: homogenous and inhomogeneous (Bloch domain walls), including also the role of spin-active interfaces at the two boundaries. In the quasiclassical framework employed here, we have to consider an exchange field much weaker than the Fermi energy in order to remain within the regime of validity. For a weak, diffusive ferromagnetic alloy such as PdNi, the exchange field  $h/\Delta_0$  can be varied from a few meV to tens of meV by changing the relative content of Pd and Ni. Even weaker exchange fields  $h$  of order meV are found in for instance  $Y_4Co_3$ ,  $Y_9Co_7$ , and  $TiBe_{1.8}Cu_{0.2}$ <sup>31</sup>. Therefore, we shall here consider exchange fields ranging from 0.5 meV up to 5 meV. The scenario of a thin junction  $d_F/\xi_S=0.3$  will be contrasted with that of a thick junction  $d_F/\xi_S = 1.0$ . For a superconducting lead like Nb with a coherence length of  $\xi_S \simeq 18$  nm, the ratio of  $d_F/\xi_S=0.3$  provides a ferromagnetic layer thickness equal to 6 nm which is experimentally accessible<sup>32</sup>. The temperature will be fixed at  $T=0.05T_c$  and consequently our results are valid for low temperature regime. The spin-dependent interfacial phase-shift (spin-DIPS) term  $G_\phi = G_S/G_T$  is obtained via the microscopic theory introduced in the previous section, and depends *e.g.* on the magnitude of the exchange field and the interface transparency. Since we calculate  $G_S$  microscopically for a simplified model with a Dirac tunneling barrier,  $G_S$  is not treated as a phenomenological parameter here. We choose  $\mu_F = 1$  eV and  $\mu_S = 10$  eV for the Fermi level in the ferromagnet and superconductor, respectively, and consider a relatively low transparency barrier of  $Z_0 = 3$ . The electron mass  $m_F$  and  $m_S$  in both of the F and S regions is taken to be the bare one ( $\simeq 0.5$  MeV). The ratio of the electronic resistances of the barrier region and the ferromagnet layer is assumed to be  $\zeta=R_B/R_F=4$  throughout our computations. We also insert a small imaginary part  $\delta=10^{-3}\times\Delta_0$  into quasiparticle energies *i.e.*  $E \rightarrow E + i\delta$  for access to more stability in our computations. The small imaginary part can be interpreted as accounting for inelastic scattering. As we discuss below, we find that the specific heat of the S|F|S diffusive junction can be strongly enhanced by changing the phase difference between the two singlet superconducting leads from 0 up to values near  $\pi$  for both a homogeneous exchange field and in the domain wall case. Due to limitations of our numerical code, we were not able to investigate phase differences  $\phi$  very close to  $\pi$ . The huge enhancement of the specific heat can be seen even for values of the exchange field several times the superconducting gap in the domain wall case. Upon increasing the magnitude of the exchange field further to values  $h \gg \Delta_0$ , this effect vanishes. The enhancement is most resilient towards an increase in  $h$  in the case where a domain wall is present. Both the enhancement of the specific heat and its persistence in the domain wall case can be understood by investigating the DOS in the ferromagnetic region. We now proceed to a presentation of our main results.

### A. Density of states (DOS) of a S|F|S junction at low temperatures

In this section, we discuss the behavior of the DOS in a ferromagnetic region by changing the phase difference between two superconducting leads connected to it. We fix the temperature at  $T=0.05T_c$  and also use from microscopically values for spin-DIPS term in the two boundaries. The results are shown in Fig. 2 for the homogeneous exchange field case, while the domain wall scenario is demonstrated in Fig. 3. In both figures, we provide a contour-plot of the DOS in the middle of the F layer as a function of quasiparticle energy  $E$  measured from Fermi level and the superconducting phase difference  $\phi$ .

Let us first consider the homogeneous case shown in Fig. 2(a) for the case  $d_F/\xi_S=0.3$  and  $h/\Delta=0.5$ . The most obvious feature is that a minigap-structure is induced in the low-energy regime close to the Fermi level, flanked by a peak structure below the gap and at the gap. The minigap is shown to close as the phase difference moves towards  $\phi = \pi$ , as is also the case for S|N|S junctions<sup>16</sup>. In Fig. 2(c), the junction thickness is increased to  $d_F/\xi_S = 1.0$ , and it is seen that the peak structures remain. The main difference from (a) is that the low-energy DOS is enhanced, indicating the odd-frequency correlations are present and comparable in magnitude to the even-frequency correlations. The minigap is split into two and is seen to shift away from zero energy. The appearance of the multiple peak structures as a function of energy  $E$  originates from an effective superconducting gap felt by each spin species which is different in magnitude for spin- $\uparrow$  and spin- $\downarrow$  quasiparticles. This is similar to the scenario of thin-film superconductors subjected to an in-plane external magnetic field<sup>33</sup>. When the exchange field is increased to  $h/\Delta_0 = 10$  as shown in (b) and (d), only the standard BCS-coherence peaks remain at the gap, although much weaker in magnitude than in the bulk case.

We now turn to the domain wall case, shown in Fig. 3. The most noteworthy change from Fig. 2 is that the zero-energy DOS is enhanced in (b) and (c). This observation signals that odd-frequency correlations are stronger in the domain-wall case, a finding which agrees with the results in Ref.<sup>27</sup>. The physical reason for this is that the inhomogeneous magnetization texture generates not only the  $S_z = 0$  triplet component, but also the long-ranged  $S_z = \pm 1$  triplet components, which also are odd in frequency due to the isotropization caused by the impurity scattering.

The presentation of the DOS and its dependence on the energy  $E$  and superconducting phase difference  $\phi$  presented in this section is a useful preliminary which, as we shall see, explains the origin behind our main result of a strongly enhanced specific heat, which we shall now move on to.

### B. Electronic specific heat of S|F|S junction at low temperatures

Let us consider the electronic specific heat of the S|F|S diffusive Josephson junction vs. phase difference of the two

superconducting leads. As mentioned in the Introduction, the phase difference is an experimentally tunable quantity by means of *e.g.* current-biasing the junction or applying an external magnetic field in a SQUID-like geometry. Since the proximity effect is in general much weaker in the low-energy regime for  $d_F/\xi_S = 1.0$ , we focus here on the more interesting case  $d_F/\xi_S=0.3$ .

The results are shown in Fig. 4. As seen, the left panel is related to the homogeneous exchange field scenario while the right panel is related to the inhomogeneous magnetization in the form of a Bloch domain wall. In both cases, the curves show a giant enhancement of the normalized specific heat when the exchange field is comparable in magnitude to the superconducting gap. For larger exchange fields, the specific heat becomes a monotonic, nearly constant function of the phase difference  $\phi$ . We note that the enhancement persists for larger values of  $h$  in the domain wall case (up to  $h/\Delta_0 \simeq 3.0$ ) compared to the homogeneous case. The physical reason behind the enhancement of the specific heat stems from the dependence of the DOS on  $\phi$ , as shown in Figs. 2 and 3. For instance, for a very weak exchange field  $h/\Delta_0 = 0.5$ , the DOS-plots presented in the previous section showed how the minigap closed with increasing  $\phi$ . Since it is the low-energy DOS that mainly contributes to the electronic specific heat, increasing the phase difference  $\phi$  will naturally lead to an increase in  $C_F$ . More specifically, we have verified numerically that at  $T/T_c=0.05$ , only energies up to  $E/\Delta_0 \simeq 0.35$  contribute to the specific heat integral in Eq. (12).

By increasing the magnitude of the exchange field in the ferromagnetic layer, a kink appears in the specific heat. To identify the cause of the appearance of the kinks, one should investigate the related DOS of the system. Consider now for concreteness the DOS in the homogeneous exchange field case with  $h/\Delta_0=1.1$ , which is seen to display a kink in the

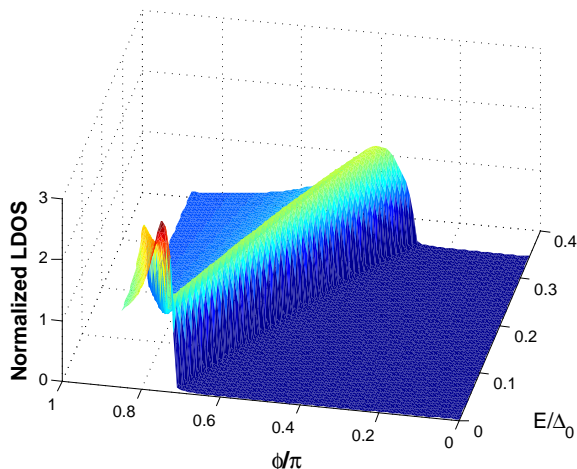


FIG. 5: (Color online) The normalized local density of states of the diffusive S|F|S junction vs. phase difference and energy for homogeneous structure of ferromagnetic layer with exchange field  $h/\Delta_0 = 1.1$  and thickness  $d_F/\xi_S = 0.3$ .

specific heat in the left panel of Fig. 4. The kink of this curve appears near  $\phi/\pi \simeq 0.7$ , consequently leading us to plot the DOS of the system near this value vs.  $E/\Delta_0$  and  $\phi/\pi$ . The resulting DOS is shown in Fig. 5. As seen, the cause of appearance of a kink near  $\phi/\pi \simeq 0.7$  is the zero-energy peak that occurs in this region of the phase difference. Such a zero-energy peak should be a direct result of the manifestation of odd-frequency correlations in the system<sup>19</sup>. In Fig. 5, it is seen that an abrupt conversion takes place at  $\phi/\pi \simeq 0.7$  along the  $E = 0$  line from a fully suppressed DOS to an enhanced value compared to the normal-state. Such an abrupt conversion was also very recently studied in Ref.<sup>34</sup>, where it was demonstrated that the conversion was associated with a transition from pure even-frequency to pure odd-frequency correlations. The simultaneous decrease of the DOS when moving away from the Fermi level results in a rapid decrease of the specific heat, thus leading to the non-monotonic behavior shown in Fig. 4.

#### IV. SUMMARY

In summary, we have considered the density of states and electronic specific heat of the diffusive S|F|S Josephson junction both for a homogeneous and inhomogeneous magnetization texture, including the role of spin-active interfaces. We find that the electronic specific heat of the S|F|S junction can be tuned to undergo a strong enhancement by increasing the phase difference between two superconducting leads. The experimental requirement for observation of this effect is that the width  $d_F$  of the ferromagnetic interlayer is considerably smaller than the superconducting coherence length (typically  $d_F$  in the range 5-10 nm), and that the exchange field is comparable in magnitude to the gap. The effect persists in the domain wall case up to exchange fields  $h/\Delta_0 \simeq 3$ , yielding  $h$  in the range 4-7 meV for a weak ferromagnetic alloy. Our prediction may be tested by *e.g.* calorimetry measurements of the Josephson junction, and the results reported here could have interesting consequences for nanoscale devices relying on an active tuning of their thermodynamic properties.

#### Acknowledgments

I. B. Sperstad and T. Yokoyama are thanked for helpful discussions. J.L. and A.S. were supported by the Research Council of Norway, Grants No. 158518/432 and No. 158547/431 (NANOMAT), and Grant No. 167498/V30 (STORFORSK).



- 
- <sup>1</sup> T. Muhge, N.N. Garifyanov, Yu.V. Goryunov, G.G. Khaliullin, L.R. Tagirov, K. Westerholt, I.A. Garifullin, and H. Zabel, *Phys. Rev. Lett.* **77**, 1857 (1996).
- <sup>2</sup> Z. Radovic, M. Ledvij, L. Dobrosavljevic-Grujic, A.I. Buzdin, and J.R. Clem, *Phys. Rev. B* **44**, 759 (1991).
- <sup>3</sup> J.S. Jiang, D. Davidovic, D.H. Reich, and C.L. Chien, *Phys. Rev. Lett.* **74**, 314 (1985).
- <sup>4</sup> A.I. Buzdin and M.Y. Kuprianov, *JETP Lett.* **53**, 321 (1991).
- <sup>5</sup> L.R. Tagirov, *Physica C* **307**, 145 (1998).
- <sup>6</sup> V.V. Ryazanov, V.A. Oboznov, A.Yu. Rusanov, A.V. Veretennikov, A.A. Golubov, and J. Aarts, *Phys. Rev. Lett.* **86**, 2427 (2001).
- <sup>7</sup> A.I. Buzdin, L.N. Bulaevskii, and S.V. Panyukov, *JETP Lett.* (35), 178 (1982).
- <sup>8</sup> A.I. Buzdin and M.Y. Kuprianov, *JETP Lett.* **52**, 487 (1990).
- <sup>9</sup> F. S. Bergeret, A. F. Volkov, and K. B. Efetov, *Phys. Rev. Lett.* **86**, 4096 (2001).
- <sup>10</sup> R. S. Keizer, S. T. B. Goennenwein, T. M. Klapwijk, G. Miao, G. Xiao, A. Gupta, *Nature* **439**, 825 (2006).
- <sup>11</sup> P. Lee, *Engineering Superconductivity*, Wiley-Interscience, New York (2001).
- <sup>12</sup> F. S. Bergeret, A. F. Volkov and K. B. Efetov, *Rev. Mod. Phys.* **77**, 1321 (2005).
- <sup>13</sup> A. I. Buzdin, *Rev. Mod. Phys.* **77**, 935 (2005).
- <sup>14</sup> F. Giazotto, T. T. Heikkilä, A. Luukanen, A. M. Savin, and J. P. Pekola, *Rev. Mod. Phys.* **78**, 217 (2006).
- <sup>15</sup> H. Rabani, F. Taddei, O. Bourgeois, R. Fazio, and F. Giazotto, *Phys. Rev. B* **78**, 012503 (2008); H. Rabani, F. Taddei, F. Giazotto, and R. Fazio, *J. Appl. Phys.* **105**, 093904 (2009).
- <sup>16</sup> J. C. Hammer, J. C. Cuevas, F. S. Bergeret,<sup>3</sup> and W. Belzig, *Phys. Rev. B* **76**, 064514 (2007).
- <sup>17</sup> H. le Sueur, P. Joyez, H. Pothier, C. Urbina, and D. Esteve, *Phys. Rev. Lett.* **100**, 197002 (2008).
- <sup>18</sup> W. L. McMillan, *Phys. Rev.* **175**, 537 (1968).
- <sup>19</sup> T. Yokoyama, Y. Tanaka, and A. A. Golubov<sup>3</sup>, *Phys. Rev. B* **75**, 134510 (2007); J. Linder, T. Yokoyama, and A. Sudbø, *Phys. Rev. B* **77**, 174514 (2008).
- <sup>20</sup> G. M. Zassenhaus *et al.*, *J. Low. Temp. Phys.* **110**, 275 (1998).
- <sup>21</sup> G. Eilenberger, *Z. Phys.* **214**, 195 (1968).
- <sup>22</sup> W. Belzig, F. K. Wilhelm, C. Bruder, G. Schön, and A. D. Zaikin, *Superlattices Microstruct.* **25**, 1251 (1999).
- <sup>23</sup> D. A. Ivanov and Ya. V. Fominov, *Phys. Rev. B* **73**, 214524 (2006).
- <sup>24</sup> N. Schopohl and K. Maki, *Phys. Rev. B* **52**, 490 (1995).
- <sup>25</sup> A. Konstandin, J. Kopu, and M. Eschrig, *Phys. Rev. B* **72**, 140501(R) (2005).
- <sup>26</sup> K. Usadel, *Phys. Rev. Lett.* **25**, 507 (1970).
- <sup>27</sup> J. Linder, T. Yokoyama, and A. Sudbø, *Phys. Rev. B* **79**, 054523 (2009).
- <sup>28</sup> D. Huertas-Hernando, Yu. V. Nazarov, and W. Belzig, *Phys. Rev. Lett.* **88**, 047003 (2002); D. Huertas-Hernando, Yu. V. Nazarov, and W. Belzig, arXiv:cond-mat/0204116.
- <sup>29</sup> A. Cottet and W. Belzig, *Phys. Rev. B* **72**, 180503 (2005).
- <sup>30</sup> A. Cottet, *Phys. Rev. B* **76**, 224505 (2007).
- <sup>31</sup> A. Kolodziejczyk *et al.*, *J. Phys. F: Met. Phys.* **14**, 1277 (1984).
- <sup>32</sup> V. A. Oboznov, V. V. Bolginov, A. K. Feofanov, V. V. Ryazanov, and A. I. Buzdin, *Phys. Rev. Lett.* **96**, 197003 (2006).
- <sup>33</sup> R. Meservey and P. M. Tedrow, *Phys. Rep.* **238**, 173 (1994).
- <sup>34</sup> J. Linder, T. Yokoyama, D. Huertas-Hernando, A. Sudbø, *Phys. Rev. Lett.* (2009).